

MARS: RESPONSE OF ICE-RICH PERMAFROST TO MILANKOVITCH FORCING AND THE ORIGIN OF THE POLAR LAYERED DEPOSITS. Norbert Schörghofer, *Institute for Astronomy, University of Hawaii, 2680 Woodlawn Drive, Honolulu, HI 96822 (norbert@hawaii.edu).*

Introduction: The Phoenix Lander touched down in the high northern latitudes of Mars and verified the presence of shallow subsurface water ice. This subsurface ice, discovered by the Gamma Ray and Neutron Spectrometer Suite poleward of about 55° latitude on both hemispheres [1, 2, 3], represents the largest ice reservoir on Mars by area. Equilibrium calculations based on exchange of water vapor between the atmosphere and the subsurface predict the geographic distribution and depth of the ice with reasonable accuracy [4, 5, 6, 7, 8, 9]. Progress in subsurface ice modeling over the past few years [10, 11] enables us to not only determine the equilibrium distribution but follow the evolution of the ice in response to temperature and climate change. Both, equilibrium and non-equilibrium models, predict that the margin (latitudinal boundary) of the two hemispheric ice layers moved over the past few million years [6, 10]. In addition to the permafrost, large volumes of water ice are found in the Polar Layered Deposits and tropical mountain glaciers [12]. By conservation of mass, any change in ice volume must be reflected in more than one of these reservoirs. Figure 1 illustrates the ice reservoirs on Mars and the exchange between the ice-rich permafrost and the Polar Layered Deposits.

A change of 1° in latitude of the subsurface ice layer margins corresponds to an area of $6 \times 10^5 \text{ km}^2$, comparable to the size of the north polar cap ($8.37 \times 10^5 \text{ km}^2$ [13]). The combined area of the polar layered terrain (north and south) is $1.8 \times 10^6 \text{ km}^2$ [13]. Below, we will estimate the thickness of the ice-rich permafrost near 60° .

The periodic nature of the Polar Layered Deposits has long led to speculations about orbital climate forcing [e.g., 14]. Subsurface ice reacts to changes in surface temperature and atmospheric humidity. Insolation is affected by the planet's axis tilt (obliquity), the eccentricity of the orbit around the sun, and the longitude of the perihelion.

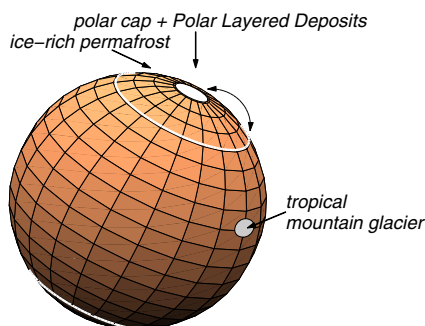


Figure 1: Ice reservoirs on Mars. The white line illustrates the margin of the ice-rich permafrost ($\sim 55^\circ$). Sublimation from the north polar cap provides vapor that can lead to the accumulation of subsurface ice, and, vice versa, retreat of the ice-rich permafrost can deposit a layer of ice on the polar cap.

Model: Explicit models of vapor diffusion and deposition are limited to numerical time steps of less than one second. The net loss and net gain of ice, but not the diurnal and seasonal variations in H_2O content, can be obtained from time-averaged transport equations, as a basis for much faster numerical methods. This method accelerates simulations by four orders of magnitude [10, 11]. The subsurface model simulates the growth of ice in interstitial soil pores from atmospherically derived water vapor and the retreat of interstitial ice. The margins are assumed to have been depleted at least once since the last precipitation, and thus there is no initial ice sheet. As ice fills the pore spaces, pathways are blocked and the growth slows, but laboratory experiments show that it can still fill a large fraction of the pore volume [15, 16]. Surface temperatures are obtained from a one-dimensional thermal balance between incoming solar light and reradiation from the surface to space with simple approximations of atmospheric absorption and emission. The bottom boundary of the subsurface ice is restricted by geothermal heat. Constant present-day atmospheric humidity is used.

Results: Figure 2 shows burial depths at 55°N and 60°N as well as at the Phoenix Landing site (68°N). At 55° , the ice changes repeatedly between stable and unstable, accumulating slowly when it is stable but retreating rapidly when it is unstable. Retreats coincide with periods of low obliquity; at this particular latitude, temperature is high when obliquity is low and vice versa. At 60° , growth is uninterrupted but not rapid enough to follow the variations in the equilibrium ice table. At the Phoenix Landing site, the ice is expected to be close to equilibrium.

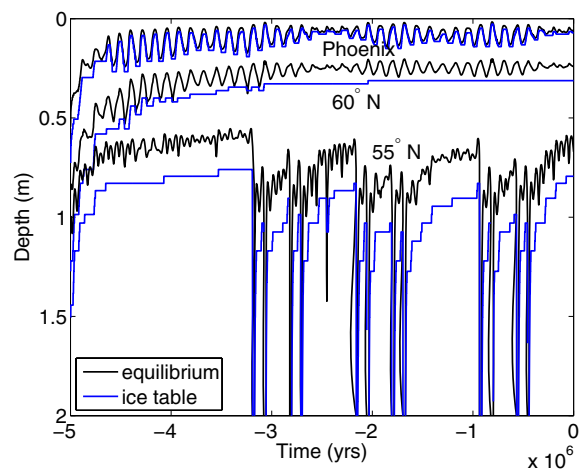


Figure 2: Depth of the equilibrium ice table (black) and the actual ice table (blue) as a function of time for three latitudes, including the Phoenix landing site. It is arbitrarily assumed that there was no ice 5 Ma ago and atmospheric humidity is constant. (The ice table depth shows the depth of the uppermost grid point with ice, leading to discrete numerical steps.)

Figure 3 shows the thickness of the ice-rich layer, i.e. the geothermally limited depth of the ice minus the depth of the ice table. At a latitude of 55° , the ice becomes repeatedly unstable and its thickness is limited by the time available for growth; it never reaches more than a few meters. At 60° , growth is uninterrupted, and the thickness increases slowly. The ice table moves upward and the bottom boundary moves downward.

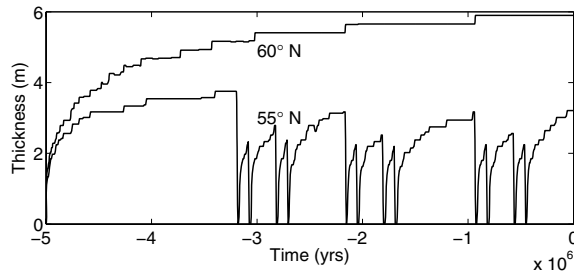


Figure 3: Thickness of ice-rich permafrost as a function of time until the present for two latitudes.

The asymptotic thickness can be estimated theoretically. Balancing of the downward pumping with the upward geothermally induced vapor transport leads to the following approximate relation,

$$T_a^2 \frac{H}{RT_m} = 2gT_m\delta_{icy},$$

where T_a is the temperature amplitude at the bottom of the icy layer, $H/(RT_m) \approx 30$, g is the geothermal temperature gradient in dry regolith (~ 0.5 K/m), T_m is mean temperature, and δ_{icy} is the seasonal skin depth in the icy layer (~ 5 m). Typical parameters lead to $T_a \approx 5$ K. The seasonal temperature amplitude on the surface may be around 20 K, such that one to two skin depths reduce the amplitude appropriately. Thus the asymptotic thickness of the ice-rich layer, where its growth is uninterrupted, should be on the order of ten meters, a value that may be asymptotically approached in Fig. 3.

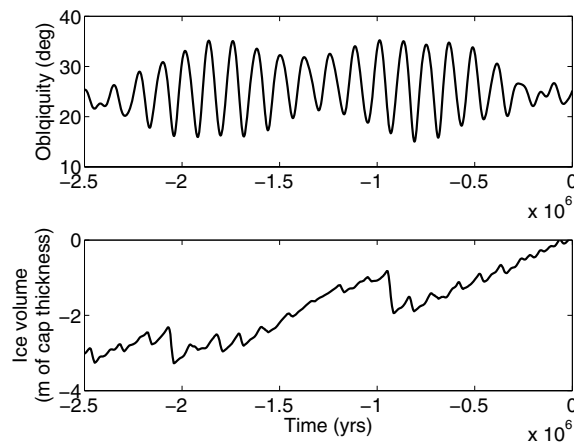


Figure 4: Subsurface ice volume at 50° - 68° N. A decrease represents loss of ice from the permafrost layer.

With this thickness, the volume changes from contraction or expansion of the ice-rich permafrost are large. Figure 4 integrates the ice volume change from latitudes 50° to 68° N and expresses it in terms of the thickness of an ice layer covering the north polar cap. A change of 1 m within 30 ka occurs about 0.9 Ma ago, and smaller changes occur in the more recent past.

After subtracting the slow overall trend, most of the volume variation arises from around 55° latitude, and less from the ice table depth changes at high latitudes, which is why the calculations emphasize the geographic area where the margin is located rather than higher latitudes. The simulation only includes the northern hemisphere ice; a similar behavior is expected for the southern hemisphere.

Mean annual surface temperature varies comparatively little at 60° N, where in the past 3 Ma it has a root-mean-square variation of only 2 K [17]. Constant atmospheric humidity likely underestimates the volume changes compared to time variable atmospheric humidity. When obliquity is low, the climate is drier and hence the retreat even faster. Additional calculations with variable humidity are being carried out. Rapid retreat will supply additional vapor to the atmosphere, which may slow the retreat. This feedback can only be considered with global coupled subsurface-atmosphere models, which are not yet available.

Conclusions: Subsurface ice retreats very rapidly when it is unstable, but near the margins the growth is slow. Retreat at the margins during periods of low obliquity involves enough ice volume to create a 1-m thick layer on the north polar cap within the last million years, based on simulations with orbitally driven surface temperature variations but constant humidity. It is plausible that the layers of the Polar Deposits can be explained in terms of contractions of the ice-rich permafrost layer.

References:

- [1] W. V. Boynton et al. *Science*, 297(5578), 81–85, 2002.
- [2] W. C. Feldman et al. *Science*, 297(5578), 75–78, 2002.
- [3] I. G. Mitrofanov et al. *Science*, 297(5578), 78–81, 2002.
- [4] R. B. Leighton & B. C. Murray. *Science*, 153, 136–144, 1966.
- [5] M. T. Mellon & B. M. Jakosky. *J. Geophys. Res.*, 98(E2), 3345–3364, 1993.
- [6] M. T. Mellon & B. M. Jakosky. *J. Geophys. Res.*, 100(E6), 11,781–11,799, 1995.
- [7] M. T. Mellon, et al. *Icarus*, 169, 324–340, 2004.
- [8] N. Schorghofer & O. Aharonson. *J. Geophys. Res.*, 110(E5), E05003, 2005.
- [9] B. Diez, et al. *Icarus*, 196(2), 409–421, 2008.
- [10] N. Schorghofer. *Nature*, 449(7159), 192–194, 2007.
- [11] N. Schorghofer. Fast numerical method for growth and retreat of subsurface ice on Mars, 2009. In preparation.
- [12] J. W. Head et al. *Nature*, 434(346–351), 2005.
- [13] H. H. Kieffer, et al. In Kieffer et al. [18], chapter 1, pages 1–33.
- [14] O. B. Toon, et al. *Icarus*, 44, 552–607, 1980.
- [15] T. L. Hudson, et al. *J. Geophys. Res.*, 2009. In press.
- [16] T. L. Hudson. *Growth, Diffusion, and Loss of Subsurface Ice on Mars: Experiments and Models*. Ph.D. thesis, Caltech, Pasadena, California, 2008.
- [17] N. Schorghofer. *Geophys. Res. Lett.*, 35, L18201, 2008.
- [18] H. H. Kieffer, et al., editors. *Mars*. Space Science Series. Univ. Arizona Press, Tucson, 1992.